GaAs Enhancement-Mode NMOSFETs Enabled by Atomic Layer Epitaxial $La_{1.8}Y_{0.2}O_3$ as Dielectric

L. Dong, X. W. Wang, J. Y. Zhang, X. F. Li, R. G. Gordon, and P. D. Ye, *Fellow, IEEE*

***Abstract*—We demonstrate high-performance enhancement-mode (E-mode) GaAs NMOSFETs with an epitaxial gate dielectric layer of $La_{1.8}Y_{0.2}O_3$ grown by atomic layer epitaxy (ALE) on GaAs(111)A substrates. A 0.5-μm-gate-length device has a record-high maximum drain current of 336 mA/mm for surface-channel E-mode GaAs NMOSFETs, a peak intrinsic transconductance of 210 mS/mm, a subthreshold swing of 97 mV/dec, and an I_{ON}/I_{OFF} ratio larger than 10^7. The thermal stability of the single-crystalline $La_{1.8}Y_{0.2}O_3$–single-crystalline GaAs interface is investigated by capacitance–voltage ($C-V$) and conductance–voltage ($G-V$) analysis. High-temperature annealing is found to be effective to reduce D_{it}.**

***Index Terms*—Atomic layer epitaxy (ALE), enhancement mode (E-mode), GaAs MOSFET.**

I. Introduction

As the device scaling and performance improving continues, silicon CMOS technology is approaching its fundamental physical limits. Meanwhile, III-V semiconductors have gained more and more attention, as they are promising candidates for replacing silicon owing to their high electron mobility and high saturation velocity [1]–[5]. During the past decades, tremendous efforts have been made to improve the oxide–GaAs interface, which is crucial for device performance [6]–[9]. However, despite some encouraging progress, the surface-channel enhancement mode (E-mode) GaAs NMOSFETs still exhibit relatively low current drivability due to the high interface trap density (D_{it}) at the oxide–GaAs interface even on (111)A substrate [9], [10]. In this letter, we demonstrate, for the first time, that, by using atomic layer epitaxy (ALE) [11], [12] to deposit the gate dielectric, high-performance GaAs surface-channel NMOSFETs can be achieved. These devices show low subthreshold slope (SS) around 97 mV/dec and high ON-state current (I_{ON}) of 336 mA/mm, which is one order of magnitude higher than that of other reported devices [9], [10]. The systematic study of C–V and $G-V$ characteristics

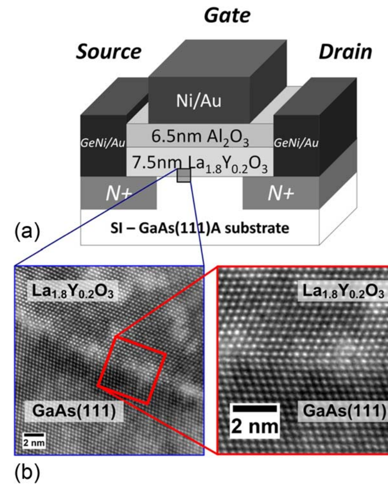

Fig. 1. (a) Cross section of a GaAs(111)A surface-channel E-mode NMOSFET. (b) HRTEM image and enlarged view of the single-crystalline GaAs–single-crystalline $La_{1.8}Y_{0.2}O_3$ interface after 860 °C RTA annealing. Epitaxial $La_{1.8}Y_{0.2}O_3$ forms a flat and sharp interface on GaAs(111)A substrate.

confirms that this novel epitaxy has an excellent quality of interface, and it is thermally stable for the fabrication process of the inversion-mode GaAs NMOSFETs.

II. Fabrication of GaAs NMOSFETs

The cross-sectional view of a GaAs(111)A NMOSFET is schematically illustrated in Fig. 1(a). The fabrication started on 2-in GaAs(111)A semi-insulating wafers. The (111)A surface is favorable for GaAs NMOSFET since it is difficult to form As–As bonds, which would pin the Fermi level in GaAs [13]. As-received GaAs wafers were first degreased by acetone, methanol, and isopropanol, and then dipped in diluted HCl to remove native oxide. Then, the wafers were soaked in 10% $(NH_4)_2S$ for 15 min at room temperature for surface passivation. After the sulfur passivation and deionized water rinse, the wafers were quickly transferred into the deposition chamber within less than 1 min for dielectric deposition. $La_{1.8}Y_{0.2}O_3$ of 7.5 nm was deposited by the ALE in this letter, followed by 6.5-nm Al_2O_3 serving as a capping layer to prevent La oxide reacting with water in air and/or during the process. The deposition of $La_{1.8}Y_{0.2}O_3$ film involves precursors of lanthanum tris(N, N′-diisopropylformamidinate), yttrium tris(N, N′-diisopropyl-acetamidinate) (from the Dow Chemical Company), and H_2O, and the deposition of Al_2O_3 used trimethylaluminium and H_2O as the precursors. The base pressure of the reactor chamber was 0.3 torr. In each cycle, the exposure

Manuscript received January 18, 2013; accepted January 25, 2013. Date of publication March 7, 2013; date of current version March 20, 2013. The work at Purdue University was supported by the Air Force Office for Scientific Research, monitored by Dr. J. C.M. Hwang. The work at Harvard University was performed at the Center for Nanoscale Systems, a member of the National Nanotechnology Infrastructure Network. The review of this letter was arranged by Editor T. Egawa.

L. Dong, J. Y. Zhang, X. F. Li, and P. D. Ye are with the School of Electrical and Computer Engineering and Birck Nanotechnology Center, Purdue University, West Lafayette, IN 47907 USA (e-mail: yep@purdue.edu).

X. W. Wang and R. G. Gordon are with the Department of Chemistry and Chemical Biology, Harvard University, Cambridge, MA 02138 USA.

Color versions of one or more of the figures in this letter are available online at http://ieeexplore.ieee.org.

Digital Object Identifier 10.1109/LED.2013.2244058

0741-3106/$31.00 © 2013 IEEE

of the La and Y precursors was 0.003 torr, and the exposure of H_2O was 0.06 torr. After each H_2O pulse, the chamber was purged under nitrogen flowing for 80 s to minimize the amount of water and/or hydroxyl groups trapped in the oxide film, as they considerably degrade the crystallinity and the permittivity. A more detailed deposition process is described elsewhere [12]. To fabricate the devices, source and drain regions were selectively implanted with a Si dose of 1×10^{14} cm^{-2} at 30 keV and 1×10^{14} cm^{-2} at 80 keV. Implantation activation was achieved by rapid thermal anneal (RTA) at 860 °C for 15 s in N_2 ambient. The source and drain areas were defined by photolithography and then covered by evaporated Au/Ge/Ni/Au metal stack. After a lift-off process, the RTA at 400 °C for 30 s in 1 atm. pressure of N_2 was performed to form ohmic contacts. The device fabrication process was completed with electron beam evaporation of Ni/Au as gate electrodes, followed by a lift-off process. The fabricated devices have a nominal gate length L_G varying from 0.5 to 40 μm, while the gate width is fixed at 100 μm. The MOS capacitors were fabricated on p-type (Zn-doped) GaAs(111)A substrates with a doping level of $5{-}7 \times 10^{17}$ cm^{-3} and n-type (Si-doped) GaAs(111)A substrates with a doping level of $6{-}9 \times 10^{17}$ cm^{-3}. The same oxide stacks of 7.5-nm $La_{1.8}Y_{0.2}O_3$/6.5-nm Al_2O_3 were used. Ni/Au as the top gate metal was used for the capacitor fabrications. Some of the oxide–GaAs stacks were annealed in N_2 prior to gate electrode formation for studying the thermal stability of the oxide–GaAs interface.

III. Results and Discussion

As shown in Fig. 1(b), the high-resolution transmission electron microscopy (HRTEM) image shows that the single-crystalline $La_{1.8}Y_{0.2}O_3$–single-crystalline GaAs (111)A interface is atomically sharp and flat, and the lattice planes are well aligned. This epitaxial structure of $La_{1.8}Y_{0.2}O_3$/GaAs was further confirmed by high-resolution X-ray diffraction (HRXRD) [12], and the lattice mismatch between $La_{1.8}Y_{0.2}O_3$ and GaAs, determined by HRXRD, is -0.67%. The output characteristics and the transfer characteristics of $L_G = 0.5$ μm GaAs(111)A NMOSFET are plotted in Fig. 2(a) and (b), respectively. The gate leakage current density is also plotted in Fig. 2(b). At a gate bias of 5 V and a drain bias of 2 V, a high maximum drain current of 336 mA/mm is achieved, which is a significant improvement of the ON-state current compared with the previously reported GaAs (111)A NMOSFETs with amorphous Al_2O_3 as the gate dielectric [10]. We believe that this is due to the novel high-quality $La_{1.8}Y_{0.2}O_3$–GaAs epitaxial interface that passivates surface dangling bonds on the GaAs surface such that the interface traps are greatly reduced. [11], [12] The peak mobility of these devices is determined to be 310 $\mathrm{cm^2/(V \cdot s)}$ at an inversion charge density of $2 \times 10^{12}/\mathrm{cm}^2$ by split-CV method. It reduces to 230 $\mathrm{cm^2/(V \cdot s)}$ at a $7 \times 10^{12}/\mathrm{cm}^2$ inversion charge density. The drive current and the channel mobility could be further enhanced using GaAs buried channel structure [7] or the incorporation of InGaAs higher mobility channel materials [3]–[5]. Our GaAs NMOSFETs also exhibit a high $I_{\mathrm{ON}}/I_{\mathrm{OFF}}$ ratio greater than 10^7 (I_{OFF} at $V_G = 0.5$ V and $V_D = 2$ V; I_{ON} at $V_G = 2.3$ V and $V_D = 2$ V). This high $I_{\mathrm{ON}}/I_{\mathrm{OFF}}$ ratio is a promising feature for GaAs as compared with InGaAs, since the latter usually suffers from high S/D leakage current as a result of its relatively narrower band gap. The NMOSFETs with any gate length fabricated in this letter (i.e., from 0.5 to 40 μm) consistently show low SS ~ 97 mV/dec, suggesting a low D_{it} value of $\sim 3.0 \times 10^{12}/\mathrm{cm}^2$-eV in the midgap using $\mathrm{SS} = 60$ mV/dec $(1 + qD_{\mathrm{it}}/C_{\mathrm{ox}})$. We notice that the gate leakage current increases from $\sim 10^{-7}$ to $\sim 10^{-3}$ A/cm^2 as the gate bias increases from 0 to 4 V, but still, the leakage current is five orders of magnitude lower than the drain current ($V_G = 4$ V). Fig. 2(c) shows the effective gate length L_{eff} and the series resistance R_{SD} extracted by plotting R_{CH} versus L_G, where R_{CH} represents the total channel resistance measured from devices with various gate lengths under gate bias from 2.5 to 4 V. R_{SD} is determined to be 2.5 $\Omega \cdot$ mm, which can be further reduced by optimizing the processes of ion implantation and S/D contact fabrication. ΔL, defined as the difference between the mask gate length L_G and L_{eff}, is estimated to be ~ 0.2 μm, due to the lateral dopant diffusion caused by high-temperature activation and/or the photolithographic misalignment. As shown in Fig. 2(d), the maximum intrinsic transconductance G_m of the $L_G = 0.5$ μm GaAs NMOSFET is $\sim$210 mS/mm after subtracting $R_{\mathrm{SD}}/2$, whereas the maximum extrinsic G_m is $\sim$138 mS/mm. G_m can be also improved by reducing the thicknesses of the $La_{1.8}Y_{0.2}O_3$ and Al_2O_3 capping layer. The equivalent oxide thickness is about 4.5 nm.

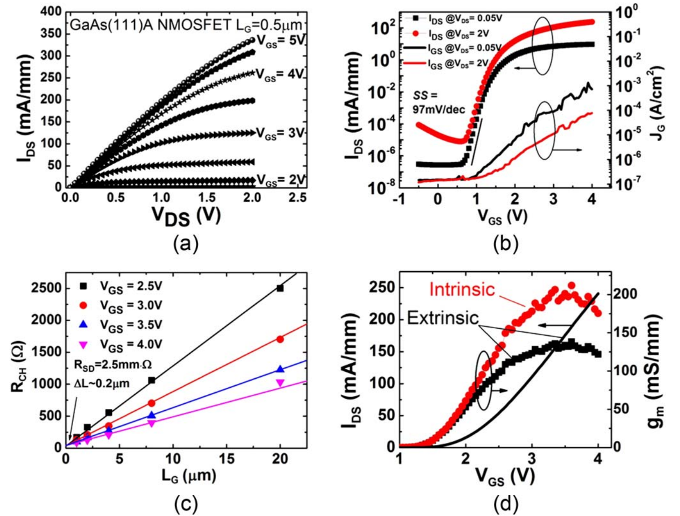

Fig. 2. (a) Current–voltage (I–V) characteristic of a 0.5-μm-gate-length GaAs NMOSFET with ALE $La_{1.8}Y_{0.2}O_3$ gate oxide. (b) Transfer characteristics and gate leakage current density of the same GaAs NMOSFET as (a). (c) Measured channel resistance versus different mask gate lengths as a function of gate bias. R_{SD} of 2.5 $\Omega \cdot$ mm and ΔL of ~ 0.2 μm are determined from the fitting lines. (d) Extrinsic and intrinsic transconductance G_m and extrinsic drain current versus gate bias of the same GaAs NMOSFET in (a).

We further investigate the thermal stability of the oxide–GaAs interface by comparing the C–V and G–V characteristics measured on samples with and without RTA treatment. Fig. 3 summarizes the C–V characteristics of n- and p-type $\mathrm{Ni/Al_2O_3/La_{1.8}Y_{0.2}O_3/GaAs(111)A}$ MOS capacitors. The annealing treatments at 600 °C and 800 °C were both performed in nitrogen ambient for 30 s. For the p-type C–V

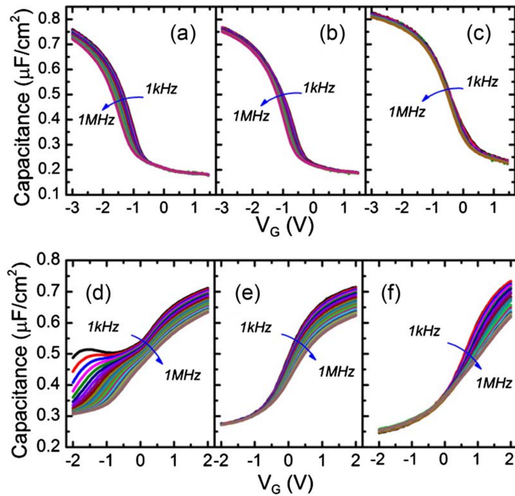

Fig. 3. C–V characteristics of the $Ni/Al_2O_3/La_{1.8}Y_{0.2}O_3/GaAs(111)A$ p- and n-type MOS capacitors of (a) and (d) as-deposited samples, (b) and (e) 600 °C annealed samples, (c) and (f) and 800 °C annealed samples. Samples b, c, e, and f were annealed in an RTA system for 30 s in nitrogen atmosphere.

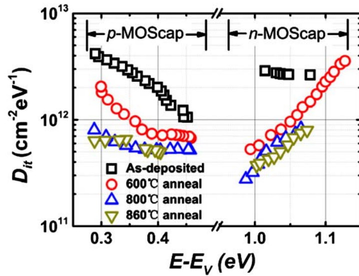

Fig. 4. D_{it} distribution in GaAs band gap obtained on p- and n-type capacitors with $La_{1.8}Y_{0.2}O_3/GaAs(111)A$ interface. The values are obtained by the conductance method at room temperature.

characteristics, the frequency dispersion at accumulation ($V_G = -3$ V) and depletion regions clearly reduced after the annealing at high temperature, which suggests that the interface trap density near the valence-band edge decreases after the RTA. Quantitatively, the frequency dispersions ($\Delta C/C_{\max}$) from 1 kHz to 1 MHz at the gate bias of -3 V measured on as-deposited, 600 °C RTA, and 800 °C RTA samples are 5%, 2.1%, and 1.8%, respectively. As for the n-type C–V characteristics, the "bump" of the capacitance caused by the high density of traps in the depletion region for the as-deposited capacitors is effectively eliminated after 600 °C or 800 °C annealing. The frequency dispersion at the depletion region is also reduced by the RTA.

We also used the conductance method to extract the D_{it} of the novel epitaxial interface. [14] The distributions of D_{it} in the GaAs band gap are summarized in Fig. 4. D_{it} for both upper- and lower-half band gaps of GaAs is effectively reduced by the high-temperature annealing, which is consistent with the C–V data shown in Fig. 3. In the lower half of the band gap, which is close to the valence-band edge, D_{it} at the position of $E - E_V = 0.35$ eV drops from 3×10^{12} $\mathrm{cm}^{-2} \cdot \mathrm{eV}^{-1}$ for the unannealed sample to 5.5×10^{11} $\mathrm{cm}^{-2} \cdot \mathrm{eV}^{-1}$ for the 800 °C and 860 °C annealed samples. Similarly, in the upper-half band gap, which is close to the conduction-band edge, at the position of $E - E_V = 1.05$ eV, D_{it} is reduced from 2.6×10^{12} $\mathrm{cm}^{-2} \cdot \mathrm{eV}^{-1}$ for the unannealed sample to 7×10^{11} $\mathrm{cm}^{-2} \cdot \mathrm{eV}^{-1}$ for the 800 °C and 860 °C annealed samples. This significant reduction of D_{it} near the conduction-band edge and also the midgap is the key to realize high-performance surface-channel GaAs NMOSFETs at epitaxial oxide/semiconductor interface.

IV. Conclusion

In summary, we have demonstrated high-performance surface-channel E-mode GaAs(111)A NMOSFETs with ALE $La_{1.8}Y_{0.2}O_3$ gate dielectric showing record-high drain current and sub-100-mV/dec subthreshold slope. We believe this high-quality epitaxial structure with excellent interface quality is very promising for future high-speed low-power logic and RF device applications.

References

[1] S. Oktyabrisky and P. D. Ye, *Fundamentals of III_V Semiconductor MOSFETs*. New York, NY, USA: Springer-Verlag, 2010.
[2] C. L. Hinkle, E. M. Vogel, P. D. Ye, and R. M. Wallace, "Interface chemistry of oxides on $In_xGa_{1-x}As$ and implications for MOSFET application," *Curr. Opin. Solid State Mater. Sci.*, vol. 15, no. 5, pp. 188–207, Oct. 2011.
[3] Y. Xuan, Y. Q. Wu, and P. D. Ye, "High-performance inversion-type enhancement-mode InGaAs MOSFET with maximum drain current exceeding 1 A/mm," *IEEE Electron Device Lett.*, vol. 29, no. 4, pp. 294–296, Apr. 2008.
[4] M. Radosavljevic, B. Chu-Kung, S. Corcoran, G. Dewey, M. K. Hudait, J. M. Fastenau, J. Kavalieros, W. K. Liu, D. Lubyshev, M. Metz, K. Millard, N. Mukherjee, W. Rachmady, U. Shah, and R. Chau, "Advanced high-k gate dielectric for high-performance short-channel $In_{0.7}Ga_{0.3}As$ quantum well field effect transistors on silicon substrate for low power logic applications," in *IEDM Tech. Dig.*, 2009, pp. 1–4.
[5] Y. Yonai, T. Kanazawa, S. Ikeda, and Y. Miyamoto, "High drain current (> 2 A/mm) InGaAs channel MOSFET at $V_D = 0.5$ V with shrinkage of channel length by InP anisotropic etching," in *IEDM Tech. Dig.*, 2011, pp. 13.3.1–13.3.4.
[6] M. Hong, J. Kwo, A. R. Kortan, J. P. Mannaerts, and A. M. Sergent, "Epitaxial cubic gadolinium oxide as a dielectric for gallium arsenide passivation," *Science*, vol. 283, no. 5409, pp. 1897–1900, Mar. 1999.
[7] R. J. W. Hill, D. A. J. Moran, L. Xu, Z. Haiping, D. Macintyre, S. Thoms, A. Asenov, P. Zurcher, K. Rajagopalan, J. Abrokwah, R. Droopad, M. Passlack, and L. G. Thayne, "Enhancement-mode GaAs MOSFETs with an $In_{0.3}Ga_{0.7}As$ channel, a mobility of over 5000 cm^2/V s, and Transconductance of Over 475 $\mu\mathrm{S}/\mu\mathrm{m}$," *IEEE Electron Device Lett.*, vol. 28, no. 12, pp. 1080–1082, Dec. 2007.
[8] H. C. Chin, M. Zhu, X. K. Liu, H. K. Lee, L. P. Shi, L. S. Tan, and Y.-C. Yeo, "Silane–ammonia surface passivation for gallium arsenide surface-channel n-MOSFETs," *IEEE Electron Device Lett.*, vol. 30, no. 2, pp. 110–112, Feb. 2009.
[9] Y. C. Wang, M. Hong, J. M. Kuo, J. P. Mannaerts, J. Kwo, H. S. Tsai, J. J. Krajewski, J. S. Weiner, Y. K. Chen, and A. Y. Cho, "Advances in GaAs MOSFETs using $Ga_2O_3(Gd_2O_3)$ as gate oxide," in *Mater. Res. Soc. Symp. Proc.*, 1999, vol. 573, p. 219.
[10] M. Xu, K. Xu, R. Contreras, M. Milojevic, T. Shen, O. Koybasi, Y. Q. Wu, R. M. Wallace, and P. D. Ye, "New insight into Fermi-level unpinning on GaAs: Impact of different surface orientations," in *IEDM Tech. Dig.*, 2009, pp. 865–868.
[11] Y. Q. Liu, M. Xu, J. Heo, P. D. D. Ye, and R. G. Gordon, "Heteroepitaxy of single-crystal $LaLuO_3$ on GaAs(111)A by atomic layer deposition," *Appl. Phys. Lett.*, vol. 97, no. 16, pp. 162910-1–162910-3, Oct. 2010.
[12] X. W. Wang, L. Dong, J. Y. Zhang, Y. Q. Liu, P. D. Ye, and R. G. Gordon, "Heteroepitaxy of La_2O_3 and $La_{2-x}Y_xO_3$ on GaAs (111)A by atomic layer deposition: Achieving low interface trap density," *Nano Lett.*, vol. 13, pp. 594–599, Feb. 2013.
[13] L. Lin and J. Robertson, "Passivation of interfacial defects at III–V oxide interfaces," *J. Vac. Sci. Technol. B*, vol. 30, no. 4, p. 04E101, Jul. 2012.
[14] G. Brammertz, K. Martens, S. Sioncke, A. Delabie, M. Caymax, M. Meuris, and M. Heyns, "Characteristic trapping lifetime and capacitance–voltage measurements of GaAs metal–oxide–semiconductor structures," *Appl. Phys. Lett.*, vol. 91, no. 13, pp. 133510-1–133510-1, Sep. 2007.